Transport coefficients for stochastic rotation dynamics in three dimensions

E. Tüzel,[1,2] M. Strauss,[3] T. Ihle,[3] and D. M. Kroll[2]
[1]*School of Physics and Astronomy, University of Minnesota, 116 Church Street SE, Minneapolis, Minnesota 55455, USA*
[2]*Supercomputing Institute, University of Minnesota, 599 Walter Library, 117 Pleasant Street SE, Minneapolis, Minnesota 55455, USA*
[3]*Institut für Computeranwendungen 1, Universität Stuttgart Pfaffenwaldring 27, 70569 Stuttgart, Germany*
(Received 25 April 2003; published 3 September 2003)

Explicit expressions for the transport coefficients of a recently introduced stochastic model for simulating fluctuating fluid dynamics are derived in three dimensions by means of Green-Kubo relations and simple kinetic arguments. The results are shown to be in excellent agreement with simulation data. Two collision rules are considered and their computational efficiency is compared.

DOI: 10.1103/PhysRevE.68.036701 PACS number(s): 47.11.+j, 05.40.−a, 02.70.Ns

I. INTRODUCTION

In a series of recent papers [1–3], a discrete-time projection operator technique was used to derive Green-Kubo relations for the transport coefficients of a new stochastic model—which we will call stochastic rotation dynamics—for simulating fluctuating fluid dynamics [4,5]. Explicit expressions for transport coefficients in two dimensions were derived, and it was shown how random shifts of the collision environment could be used to ensure Galilean invariance for arbitrary Mach number and temperature. In this paper, we extend our analytical and numerical analysis to three dimensions and consider two distinct collision rules. Expressions for the transport coefficients are derived and compared with simulation results. No assumptions are made regarding molecular chaos, and the correlations that can develop at small mean free path are explicitly accounted for. The only approximation we make is to neglect fluctuations in the number of particles in the cells which are used to define the collision environment. This amounts to neglecting terms of order e^{-M}, where M is the average number of particles in a cell, and is therefore justified in all practical calculations, where $M \geqslant 5$.

In the stochastic rotation dynamics (SRD) algorithm, the fluid is modeled by particles whose position coordinates $\mathbf{r}_i(t)$ and velocities $\mathbf{v}_i(t)$ are continuous variables. The system is coarse grained into cells of a regular lattice, and there is no restriction on the number of particles in a cell. The evolution of the system consists of two steps: streaming and collision. In the streaming step, all particles are simultaneously propagated a distance $\mathbf{v}_i\tau$, where τ is the value of the discretized time step. For the collision step, particles are sorted into cells, and they interact only with members of their own cell. Typically, the simplest cell construction consisting of a hypercubic grid with mesh size a is used. As discussed in Refs. [1] and [2], a random shift of the particle coordinates before the collision step is required to ensure Galilean invariance. In our implementation of this procedure, all particles are shifted by the *same* random vector with components in the interval $[-a/2,a/2]$ before the collision step. Particles are then shifted back to their original positions after the collision. If we denote the cell coordinate of the shifted particle i by $\boldsymbol{\xi}_i^s$, the dynamics is summarized by

$$\mathbf{r}_i(t+\tau) = \mathbf{r}_i(t) + \tau \mathbf{v}_i(t), \tag{1}$$

$$\mathbf{v}_i(t+\tau) = \mathbf{u}[\boldsymbol{\xi}_i^s(t+\tau)] + \boldsymbol{\omega}[\boldsymbol{\xi}_i^s(t+\tau)] \cdot \{\mathbf{v}_i(t) - \mathbf{u}[\boldsymbol{\xi}_i^s(t+\tau)]\}, \tag{2}$$

where $\boldsymbol{\omega}(\boldsymbol{\xi}_i^s)$ denotes a stochastic rotation matrix, and $\mathbf{u}(\boldsymbol{\xi}_i^s) \equiv (1/M)\Sigma_{k \in \boldsymbol{\xi}^s} \mathbf{v}_k$ is the mean velocity of the particles in cell $\boldsymbol{\xi}^s$. All particles in the cell are subject to the same rotation, but the rotations in different cells are statistically independent. There is a great deal of freedom in how the rotation step is implemented, and any stochastic rotation matrix consistent with detailed balance can be used. The dynamics of the SRD algorithm is explicitly constructed to conserve mass, momentum, and energy, and the collision process is the simplest consistent with these conservation laws. The algorithm is Galilean invariant, there is an H-theorem, and it yields the correct hydrodynamics equations with an ideal gas equation of state [2,4]. SRD has been used to study flow around solid objects in both two [6,7] and three [8] dimensions, dilute polymer solutions [9], binary mixtures [10,11], amphiphilic mixtures [12–14], colloids [15,16], and cluster structure and dynamics [17].

In two dimensions, the stochastic rotation matrix $\boldsymbol{\omega}$ is typically taken to be a rotation by an angle $\pm\alpha$, with probability 1/2. Analytic expressions for the transport coefficients in this case were derived in Refs. [1–3] and shown to be in excellent agreement with simulation results. In three dimensions, one collision rule that has been discussed in the literature [4,5,8] consists of rotations by an angle α about a randomly chosen direction. All orientations of the random axis occur with equal probability. Note that rotations by an angle $-\alpha$ do not need to be considered, since this amounts to a rotation by an angle α about an axis with the opposite orientation. The viscosity of this model has been measured using a Poiseuille flow geometry in Ref. [8]. Analytical expressions for the transport coefficients in this case are only available in the limit of large mean free path, $\lambda/a \to \infty$, and for one rotation angle $\alpha = 90°$ [5]. In the following, we will refer to this collision rule as model A. Another, computationally simpler collision rule, which we will refer to as model B, involves rotations about one of three orthogonal rotation

axes. In the implementation considered here, we take these to be x, y, and z axes of a Cartesian coordinate system. At each collision step one of these three axes is chosen at random, and a rotation by an angle $\pm\alpha$ is then performed, where the sign is chosen at random. This procedure is fast and easy to implement; furthermore, only six different rotation matrices are needed, which are sparse and contain fixed elements of 1, $\pm\sin(\alpha)$, and $\cos(\alpha)$. Our simulations have shown that both collision rules lead to a rapid relaxation to thermal equilibrium characterized by the Maxwell-Boltzmann velocity distribution.

The outline of the paper is as follows. In Sec. II we briefly summarize the Green-Kubo relations for the transport coefficients. Sections III and IV contain detailed descriptions of the two collision rules, as well as analytical and numerical calculations of the shear viscosity, thermal diffusivity, and self-diffusion coefficient at both large and small mean free paths. The work is summarized in Sec. V.

II. HYDRODYNAMICS

The transport coefficients of a simple liquid are the kinematic shear and bulk viscosities, ν and γ, and the thermal diffusivity coefficient D_T. Explicit expressions for the asymptotic (long-time limit) shear and bulk viscosities and thermal diffusivity of the SRD algorithm were derived in Ref. [2] using a projection operator technique. In particular, it was shown that the kinematic viscosities can be expressed in terms of the reduced fluxes in k space as

$$\nu\left(\delta_{\beta\varepsilon}+\frac{d-2}{d}\frac{k_\beta k_\varepsilon}{k^2}\right)+\gamma\frac{k_\beta k_\varepsilon}{k^2}=\frac{\tau}{Nk_BT}\sum_{t=0}^{\infty}{}'\langle I_{1+\beta}(\hat{\mathbf{k}},0)|I_{1+\varepsilon}(\hat{\mathbf{k}},t)\rangle, \quad (3)$$

while the thermal diffusivity is given by

$$D_T=\frac{\tau}{c_pNk_BT^2}\sum_{t=0}^{\infty}{}'\langle I_{d+2}(\hat{\mathbf{k}},0)|I_{d+2}(\hat{\mathbf{k}},t)\rangle, \quad (4)$$

where d is the spatial dimension, $c_p=(d+2)k_B/2$ is the specific heat per particle at constant pressure, and the prime on the sum indicates that the $t=0$ term has the relative weight 1/2. Here and in the following we have set the particle mass equal to 1. The thermal conductivity κ is related to D_T by

$$\kappa=\rho c_pD_T. \quad (5)$$

The reduced fluxes in Eqs. (3) and (4) are (see Refs. [2,3] for details)

$$I_{1+\beta}(\hat{\mathbf{k}},t)=\frac{1}{\tau}\sum_i\left(-[v_{i\beta}(t)\hat{\mathbf{k}}\cdot\Delta\boldsymbol{\xi}_i(t)+\Delta v_{i\beta}(t)\hat{\mathbf{k}}\cdot\Delta\boldsymbol{\xi}_i^s(t)]+\frac{\tau\hat{k}_\beta}{d}v_i^2(t)\right), \quad (6)$$

for $\beta=1,\ldots,d$, and

$$I_{d+2}(\hat{\mathbf{k}},t)=\frac{1}{\tau}\sum_i\left(-\left[[v_i^2(t)/2-c_vT]\hat{\mathbf{k}}\cdot\Delta\boldsymbol{\xi}_i(t)+\frac{1}{2}\Delta v_i^2(t)\hat{\mathbf{k}}\cdot\Delta\boldsymbol{\xi}_i^s(t)\right]+\tau k_BT\hat{\mathbf{k}}\cdot\mathbf{v}_i(t)\right), \quad (7)$$

where $c_v=d\,k_B/2$ is the specific heat per particle at constant volume of an ideal gas, $\Delta v_j^2=v_j^2(t+\tau)-v_j^2(t)$, $\Delta\boldsymbol{\xi}_i(t)=\boldsymbol{\xi}_i(t+\tau)-\boldsymbol{\xi}_i(t)$, and $\Delta\boldsymbol{\xi}_i^s(t)=\boldsymbol{\xi}_i(t+\tau)-\boldsymbol{\xi}_i^s(t+\tau)$, where $\boldsymbol{\xi}_i(t+\tau)$ is the cell coordinate of particle i at time $t+\tau$ and $\boldsymbol{\xi}_i^s(t+\tau)$ is the corresponding shifted particle cell coordinate. Since $\Delta\mathbf{r}_i(t)=\tau\mathbf{v}_j(t)$, $I_1(\hat{\mathbf{k}},t)=0$ to this order in k.

1. Shear viscosity

In three dimensions, the shear viscosity can be obtained if, for example, one takes $\hat{\mathbf{k}}$ in the z direction and $\beta=\epsilon=1$, in the Green-Kubo relation, Eq. (3), so that

$$\nu=\frac{\tau}{Nk_BT}\sum_{t=0}^{\infty}{}'\langle I_2(\hat{\mathbf{z}},0)|I_2(\hat{\mathbf{z}},t)\rangle. \quad (8)$$

There are two contributions to the reduced fluxes, namely, kinetic and rotational, so that

$$I_2(\hat{\mathbf{z}},t)=I_2^{kin}(\hat{\mathbf{z}},t)+I_2^{rot}(\hat{\mathbf{z}},t), \quad (9)$$

where

$$I_2^{kin}(\hat{\mathbf{z}},t)=-\frac{1}{\tau}\sum_i v_{ix}(t)\Delta\xi_{iz}(t) \quad (10)$$

and

$$I_2^{rot}(\hat{\mathbf{z}},t)=-\frac{1}{\tau}\sum_i\Delta v_{ix}(t)\Delta\xi_{iz}^s(t). \quad (11)$$

Contributions to I_2^{kin} come from the streaming step, whereas the collisions and shifts contribute to I_2^{rot}. There are corresponding kinetic, rotational, and mixed contributions to the shear viscosity.

2. Thermal diffusivity

Similarly, setting $d=3$ and taking $\hat{\mathbf{k}}$ in the z direction in Eq. (4), one has

$$D_T=\frac{\tau}{c_pNk_BT^2}\sum_{t=0}^{\infty}{}'\langle I_5(\hat{\mathbf{z}},0)|I_5(\hat{\mathbf{z}},t)\rangle. \quad (12)$$

Again, the reduced flux can be divided into the kinetic and rotational contributions, so that

$$I_5(\hat{\mathbf{z}},t)=I_5^{kin}(\hat{\mathbf{z}},t)+I_5^{rot}(\hat{\mathbf{z}},t), \quad (13)$$

where

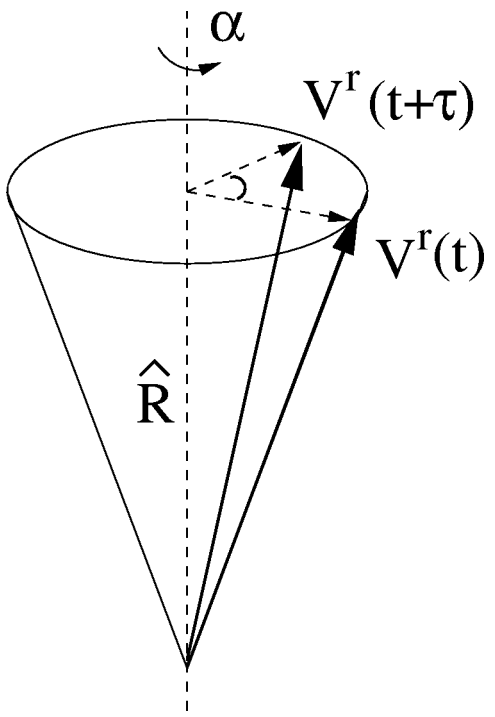

FIG. 1. Rotation of the vector $\mathbf{v}^r$ around a random direction $\hat{\mathbf{R}}$ by the angle α.

$$I_5^{kin}(\hat{\mathbf{z}},t)=\frac{1}{\tau}\sum_i\left\{\left(c_vT-\frac{v_i^2(t)}{2}\right)\Delta\xi_{iz}(t)+\tau k_BTv_{iz}(t)\right\} \tag{14}$$

and

$$I_5^{rot}(\hat{\mathbf{z}},t)=-\frac{1}{\tau}\sum_i\frac{1}{2}\Delta v_j^2(t)\Delta\xi_{iz}^s(t). \tag{15}$$

III. MODEL A: ROTATION AROUND A RANDOM AXIS

As discussed in the Introduction, one choice of collision rule is a rotation by an angle α about a randomly chosen axis (see Fig. 1). This collision rule has been used in a recent study of Poiseuille flow and flow around a spherical obstacle, and was shown to yield excellent results [8]. Denote the random vector by $\hat{\mathbf{R}}$; the postcollision velocity of a particle at time step $t+\tau$ can then be written as

$$\mathbf{v}(t+\tau)=\mathbf{u}_{\xi^s}(t)+\mathbf{v}_\perp^r(t)\cos(\alpha)+[\mathbf{v}_\perp^r(t)\times\hat{\mathbf{R}}]\sin(\alpha)+\mathbf{v}_\parallel(t), \tag{16}$$

where $\perp$ and $\parallel$ denote the components of a vector that are perpendicular and parallel to the random axis $\hat{\mathbf{R}}$; the relative velocity $\mathbf{v}^r(t)=\mathbf{v}(t)-\mathbf{u}_{\xi^s}(t)$.

The relaxation to thermal equilibrium is characterized by the decay rate of the H-function [2]. However, a simpler procedure is to monitor the relaxation of the fourth moment, $S_4=\Sigma_i(v_{ix}^4+v_{iy}^4+v_{iz}^4)$, of the velocity distribution. This was done in Ref. [2] in two dimensions, where it was shown that S_4 relaxes exponentially to the equilibrium value given by the Maxwell-Boltzmann distribution with a relaxation time

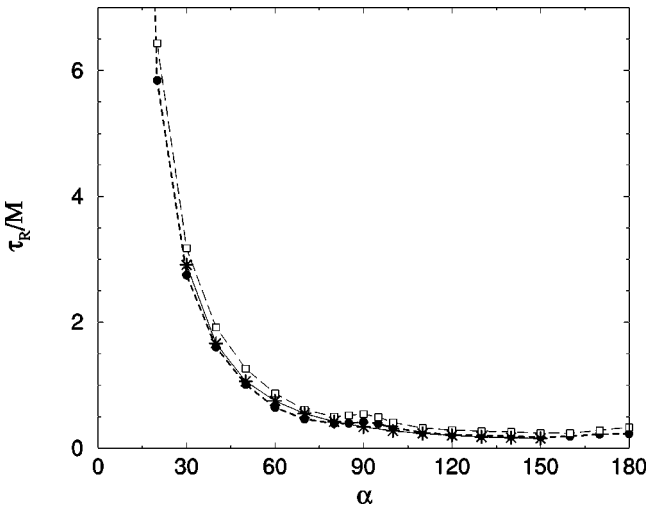

FIG. 2. The normalized relaxation time τ_R/M of the fourth moment of the velocity distribution, $S_4=\Sigma_i(v_{ix}^4+v_{iy}^4+v_{iz}^4)$ as a function of the rotation angle α for $M=20$, where M is the average number of particles per cell. The data for model A (*) were obtained for $\lambda/a=1.15$, while the data for model B correspond to $\lambda/a=1.15$ (●) and $\lambda/a=0.0361$ (□). Parameters: $L/a=32$ and $\tau=1$.

τ_R, which is essentially temperature independent. Furthermore, it was found that τ_R is proportional to the average number of particles in a cell, M, and depends strongly on the value of the rotation angle α. It diverges approximately as $\tau_R\sim\alpha^{-2}$ for $\alpha\to0$, since there are no collisions in this limit, and thermal equilibrium cannot be achieved. As can be seen in Fig. 2, similar behavior is observed in three dimensions for both models A and B.

A. Large mean free path approximation

1. Shear viscosity

For large mean free path, $\lambda/a\to\infty$, the rotational contributions to the reduced flux, $I_2^{rot}(\hat{\mathbf{z}},t)$, in Eq. (9) can be neglected, so that the shear viscosity can be expressed as

$$\nu=\frac{\tau}{Nk_BT}\sum_{n=0}^{\infty}{}'C_n, \tag{17}$$

where

$$C_n\equiv\langle I_2^{kin}(\hat{\mathbf{z}},0)|I_2^{kin}(\hat{\mathbf{z}},n\tau)\rangle$$
$$=\frac{1}{\tau^2}\sum_{ij}\langle v_{ix}(0)\Delta\xi_{iz}(0)v_{jx}(n\tau)\Delta\xi_{jz}(n\tau)\rangle. \tag{18}$$

As discussed in Ref. [3], except for the $t=0$ contribution, C_0, it is a good approximation to replace $\Delta\xi_{iz}$ by τv_{iz} when evaluating C_n. In the following, we therefore first evaluate ν using this approximation, and then discuss the required correction term.

The relevant components of Eq. (16) can be written as

$$v_{ix}(t+\tau)=u_{\xi x}(t)+c\Big[v_{ix}(t)-u_{\xi x}(t)-\sum_{\beta}[v_{i\beta}(t)-u_{\xi\beta}(t)]R_\beta R_x\Big]+s\{[v_{iy}(t)-u_{\xi y}(t)]R_z-[v_{iz}(t)-u_{\xi z}(t)]R_y\}+\sum_{\beta}[v_{i\beta}(t)-u_{\xi\beta}(t)]R_\beta R_x, \tag{19}$$

$$v_{iz}(t+\tau)=u_{\xi z}(t)+c\Big[v_{iz}(t)-u_{\xi z}(t)-\sum_{\beta}[v_{i\beta}(t)-u_{\xi\beta}(t)]R_\beta R_z\Big]+s\{[v_{ix}(t)-u_{\xi x}(t)]R_y-[v_{iy}(t)-u_{\xi y}(t)]R_x\}+\sum_{\beta}[v_{i\beta}(t)-u_{\xi\beta}(t)]R_\beta R_z, \tag{20}$$

where $c=\cos(\alpha)$, $s=\sin(\alpha)$, $\mathbf{u}_\xi=(1/M)\Sigma_{k\in\xi}\mathbf{v}_k$, and the sum runs over all particles in the cell occupied by particle i at $t=n\tau$. Defining

$$A_n=\sum_{ij}\langle v_{ix}(0)v_{iz}(0)v_{jx}(n\tau)v_{jz}(n\tau)\rangle, \tag{21}$$

we have

$$A_0=\sum_{ij}\langle v_{ix}v_{iz}v_{jx}v_{jz}\rangle=\sum_{i}\langle v_{ix}v_{iz}v_{ix}v_{iz}\rangle=N(k_BT)^2, \tag{22}$$

so that there are only contributions from $j=i$. The second term in the series is

$$A_1=\sum_{ij}\langle v_{ix}v_{iz}v_{jx}(\tau)v_{jz}(\tau)\rangle, \tag{23}$$

where $v_{jx}(\tau)$ and $v_{jz}(\tau)$ are given by Eqs. (19) and (20), respectively. There are both diagonal ($j=i$) and off-diagonal ($j\neq i$) contributions to A_1. Making use of the following averages over the random vector $\hat{\mathbf{R}}$:

$$\langle R_\beta^2\rangle=1/3 \tag{24}$$

and

$$\langle R_\beta^2R_{\beta'}^2\rangle=1/15+2/15\delta_{\beta,\beta'}, \tag{25}$$

the diagonal contribution is found to be

$$\langle v_{ix}v_{iz}v_{ix}(\tau)v_{iz}(\tau)\rangle=(k_BT)^2\zeta_A, \tag{26}$$

where

$$\zeta_A=\frac{1}{3}\left\{\left[c^2-s^2+\frac{2}{5}(c-1)^2\right]\left(\frac{1}{M}-1\right)^2+2c\left(1-\frac{1}{M^2}\right)+\frac{1}{M}\left(2+\frac{1}{M}\right)\right\}. \tag{27}$$

The off-diagonal contribution comes from particles j which are in the same cell as particle i at $t=0$. This contribution is equal to

$$\langle v_{ix}v_{iz}v_{jx}(\tau)v_{iz}(\tau)\rangle=\eta_A, \tag{28}$$

where

$$\eta_A=\frac{2}{15M^2}(6c-1)(c-1). \tag{29}$$

Since there are $M-1$ off-diagonal contributions, it follows that

$$A_1=N(k_BT)^2[\zeta_A+(M-1)\eta_A]. \tag{30}$$

The behavior over longer time intervals can be analyzed in a similar fashion. Consider A_2. Following the arguments of the last paragraph, there is a diagonal contribution proportional to ζ_A^2, and an off-diagonal contribution proportional to $2(M-1)\eta_A\zeta_A$, since at each time step, $M-1$ particles become correlated with particle i, and particle j can become correlated with particle i at either of the two time steps. Note, however, there are now additional—higher order—contributions that arise, for example, when particle j becomes correlated with particle k which then becomes correlated with particle i. It is easy to see that these contributions carry additional factors of $1/M$ and are thus of higher order than the diagonal and direct off-diagonal contributions considered above. However, these higher off-diagonal contributions can be summed in the geometric series

$$A_n/N(k_BT)^2=[\zeta_A+(M-1)\eta_A]^n\approx\zeta_A^n+n(M-1)\eta_A\zeta_A^{n-1}+\cdots, \tag{31}$$

so that

$$\nu=k_BT\tau\left(\frac{1}{2}+\sum_{j=1}^{\infty}[\zeta_A+(M-1)\eta_A]^j\right)=\frac{k_BT\tau}{2}\left(\frac{5}{\left(1-\frac{1}{M}\right)[2-\cos(\alpha)-\cos(2\alpha)]}-1\right). \tag{32}$$

As discussed above, there is an additional finite cell size correction to this result. It arises from the fact that the substitution $\Delta\xi_{iy}=\tau v_{iy}$ in C_0 is not precisely correct. Rather, it can be shown that [3]

$$C_0 \approx A_0 + N\frac{k_B T}{6}\frac{a_2}{\tau} = N(k_B T)^2\left[1+\frac{1}{6}(a/\lambda)^2\right] \quad (33)$$

for $\lambda \gg a$. Using this result in Eq. (17), the corrected kinematic viscosity is

$$\nu = \frac{k_B T \tau}{2}\left(\frac{5}{\left(1-\frac{1}{M}\right)[2-\cos(\alpha)-\cos(2\alpha)]}-1\right)+\frac{a^2}{12\tau}. \quad (34)$$

Note that although this additional term is, in general, negligibly small in three dimensions, it can dominate the viscosity in two dimensions [3]. In particular, for $M\to\infty$, the viscosity in model A takes the minimum value

$$\nu^A_{min} = \tau k_B T\left[\frac{3}{10}+\frac{1}{12}\left(\frac{a}{\lambda}\right)^2\right] \quad (35)$$

at $\alpha \approx 104.48°$. In contrast, in two dimensions, the minimum is at $\alpha = 90°$ for $M\to\infty$, and

$$\nu^{2d}_{min} = \frac{\tau k_B T}{12}\left(\frac{a}{\lambda}\right)^2. \quad (36)$$

In this limit, the finite cell size correction provides the sole contribution to the viscosity in two dimensions. The viscosity for model A is always larger than the viscosity in two dimensions. In order to determine the accuracy of Eq. (34), we have performed simulations using a system of linear dimension $L/a = 32$, using $\tau = 1$, and $M = 5$ and 20 particles per cell. Figure 3(a) contains a plot of the normalized correlation function $\langle I_2(0)I_2(t)\rangle/N(k_B T)^2$ as a function of time for two different collision angles, $\alpha = 30°$ and 150°. As expected, the correlations decay much faster for the larger collision angle. The resulting time dependent kinematic viscosity is shown in Fig. 3(b), and the normalized asymptotic value of the viscosity, $\nu/(\tau k_B T)$, is plotted in Fig. 4(a) as a function of α for $\lambda/a = 2.309$, and $M = 5$ and 20, and in Fig. 4(b) for $\lambda = 1.02$ and $M = 20$. The agreement between the analytical result and simulation data is excellent. Figure 5(a) contains a plot of the normalized kinematic viscosity $\nu\tau/a^2$ as a function of $(\lambda/a)^2$ for $\alpha = 90°$ and $M = 20$. Also shown in Fig. 5(a) are data (●) for the viscosity obtained by fitting the one-dimensional velocity profile of forced flow between parallel plates in three dimensions [8]. Again, the agreement between both sets of data and theory is excellent.

2. Thermal diffusivity

As discussed in the preceding section, for large mean free path, the rotational contributions to the thermal diffusivity in Eq. (12) can be neglected. Furthermore, finite cell size corrections of the type discussed in the preceding section do not occur in the calculation of the thermal diffusivity, so that $\Delta\xi_{iz}$ can be replaced by τv_{iz}. The thermal diffusivity can therefore be expressed as

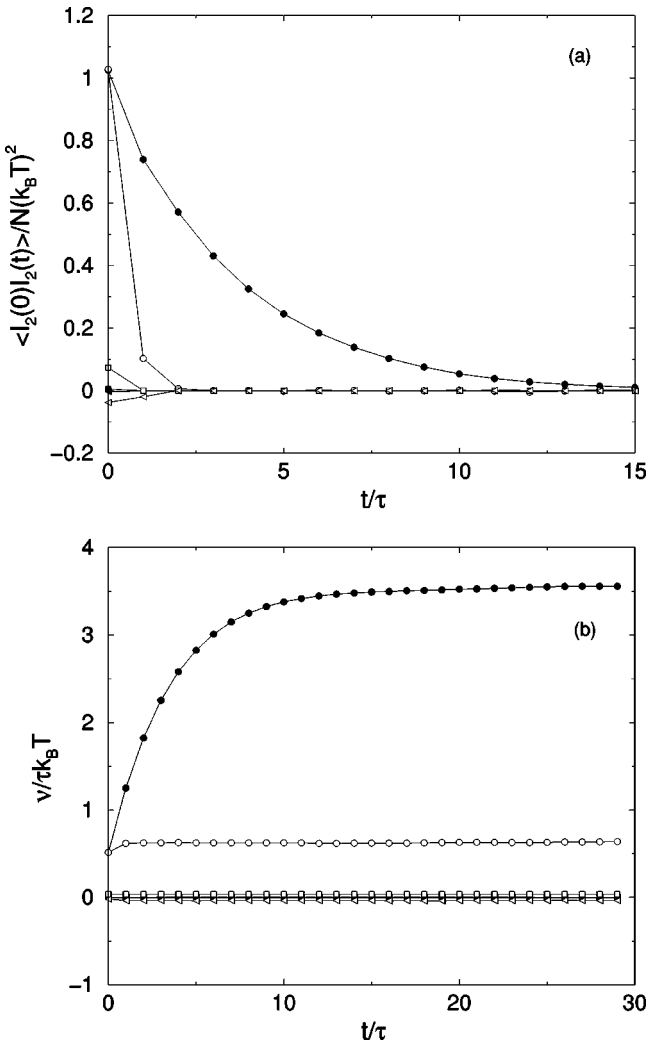

FIG. 3. (a) Normalized correlation functions $\langle I_2(0)I_2(t)\rangle/N(k_B T)^2$ for model A as a function of time for $\alpha = 30°$ (solid symbols) and $\alpha = 150°$ (unfilled symbols). For $\alpha = 30°$, the kinetic, rotational, and mixed contributions are indicated by ●, ■, and ◀, respectively. For $\alpha = 150°$, the kinetic, rotational, and mixed contributions are indicated by ○, □, and ◁, respectively. (b) Normalized time dependent kinematic viscosity, $\nu(t)/\tau k_B T$. Symbols are the same as in part (a). Parameters: $L/a = 32$, $\lambda/a = 2.309$, $\tau = 1$, and $M = 20$. The data were obtained by time averaging over 75 000 iterations.

$$D_T = \frac{\tau}{c_p N k_B T^2}\sum_{n=0}^{\infty}{}' B_n, \quad (37)$$

where $B_n \equiv \langle I_5^{kin}(\hat{\mathbf{z}},0)|I_5^{kin}(\hat{\mathbf{z}},n\tau)\rangle$ with

$$I_5^{kin}(\hat{z},t) = \sum_{i=1}^{N}\left(c_p T - \frac{v_i^2(t)}{2}\right)v_{iz}. \quad (38)$$

Since

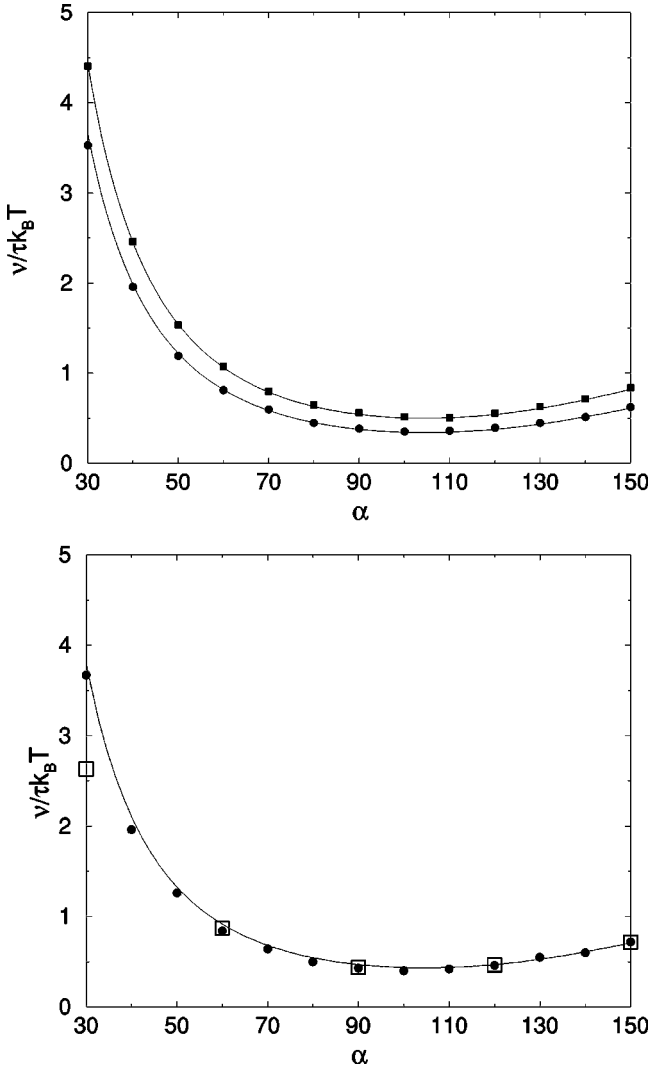

FIG. 4. Normalized kinematic viscosity $\nu/\tau k_B T$ for model A as a function of the collision angle α. (a) Data for $L/a=32$, $\lambda/a=2.309$, $\tau=1$, and $M=5$ (■) and $M=20$ (●). (b) Data for $L/a=32$, $\lambda/a=1.02$, $\tau=1$, and $M=20$. The bullets are results obtained using the Green-Kubo relation, and the unfilled boxes (□) are data for the kinematic viscosity obtained in Ref. [8] by fitting the one-dimensional velocity profile of forced flow between parallel plates. The lines are the theoretical prediction, Eq. (34), for the corresponding parameter values. The data were obtained by time averaging over 75 000 iterations. The deviation of the data point □ at $\alpha=30°$ is due to finite Knudsen number effects.

$$\left\langle c_p T\left(c_p T-\frac{v_i^2}{2}\right)v_{iz}v_{jz}(n\tau)\right\rangle=0 \tag{39}$$

for any value of n, it can be shown that

$$B_0=\frac{5}{2}N(k_BT)^3. \tag{40}$$

The next term in the series is

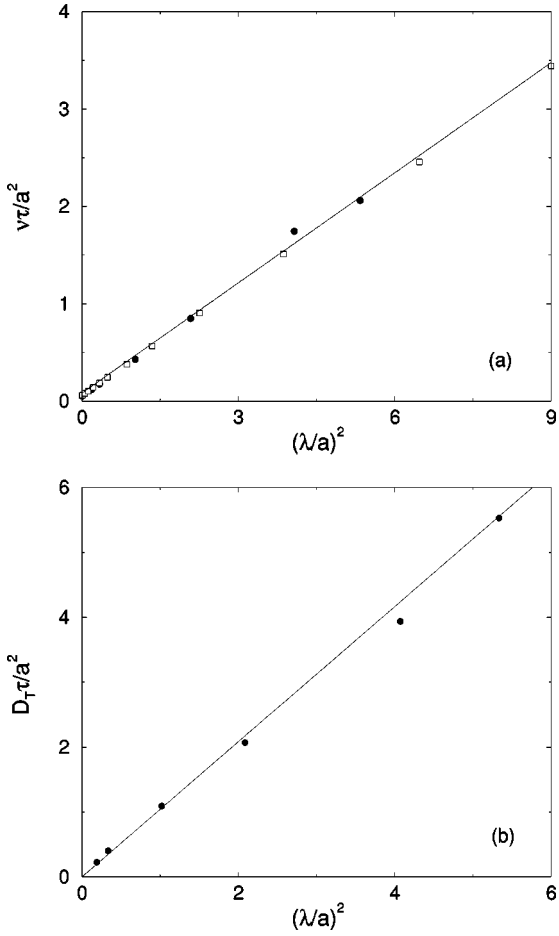

FIG. 5. (a) Normalized kinematic viscosity $\nu\tau/a^2$ and (b) thermal diffusivity $D_T\tau/a^2$ for model A as functions of $(\lambda/a)^2$ for collision angle $\alpha=90°$. The bullets are data obtained using Green-Kubo relations. The unfilled boxes (□) are data for the kinematic viscosity obtained in Ref. [8] by fitting the one-dimensional velocity profile of forced flow between parallel plates. The solid line is the theoretical prediction, Eqs. (34) and (48). Parameters: $L/a=32$, $\tau=1$, and $M=20$. The data were obtained by time averaging over 75 000 iterations.

$$B_1=\frac{N}{4}\langle v_i^2 v_i^2(\tau)v_{iz}(\tau)v_{iz}\rangle-\frac{Nc_pT}{2}\langle v_i^2(\tau)v_{iz}(\tau)v_{iz}\rangle. \tag{41}$$

In Appendix A it is shown using quaternion algebra that

$$B_1=\frac{5}{2}N(k_BT)^3\Theta, \tag{42}$$

where

$$\Theta=\left(\frac{\gamma_1}{3}+\frac{\gamma_2}{3M}\left[1-\frac{2}{M}\right]+\frac{\gamma_3}{15M^3}\right) \tag{43}$$

and

$$\gamma_1=(1+2c), \tag{44}$$

$$\gamma_2=\frac{2}{5}(c-1)(8c-3), \tag{45}$$

$$\gamma_3=\frac{128}{5}(1-c)^2. \tag{46}$$

Using quaternion algebra (see Appendix B), it can be shown in the $M\to\infty$ limit that the sum in Eq. (37) is a geometric series. Furthermore, direct calculations in two dimensions [3] and for model B (see Sec. IV A 1) suggest that this remains true in general. Assuming this is true here, the diagonal contributions to the thermal diffusivity are given by

$$B_n=\frac{5}{2}N(k_BT)^3\Theta^n, \tag{47}$$

so that carrying out the sum in Eq. (37),

$$D_T=k_BT\,\tau\left(\frac{1}{2}+\sum_{j=1}^{\infty}\Theta^j\right)$$

$$=\frac{k_BT\,\tau}{2}\left(\frac{75M^3\csc^2(\alpha/2)}{2\{-64+5M(6+M[-3+5M])+8(8+5[-2+M]M)\cos(\alpha)\}}-1\right) \tag{48}$$

$$=k_BT\,\tau\left[\frac{1}{2}\left(\frac{2+\cos(\alpha)}{1-\cos(\alpha)}\right)+\frac{3}{M}\left(\frac{4}{5}-\frac{1}{4}\csc^2(\alpha/2)\right)+O\left(\frac{1}{M^2}\right)\right]. \tag{49}$$

Data for the normalized thermal diffusivity $D_T\tau/a^2T$ as a function of $(\lambda/a)^2$ for $\alpha=90°$ and $M=20$ are compared with Eq. (48) in Fig. 5(b). The agreement is excellent. Figure 6(a) contains a plot of the various contributions to the time dependent correlation function $2\langle I_5(0)I_5(t)\rangle/5N(k_BT)^3$, and Fig. 6(b) shows the corresponding data for the time dependent thermal diffusivity for $\alpha=30°$ (filled symbols) and $\alpha=150°$ (unfilled symbols). Note that for large collision angles, stress correlations decay very rapidly, so that only the first couple of terms in the time series are needed. Finally, the normalized thermal diffusivity $D_T/\tau k_BT$ is plotted as a function of the collision angle in Fig. 7 for $M=5$ and $M=20$. Again, the results are in excellent agreement with theory. It should be emphasized that only the diagonal contributions to D_T have been considered here. Although off-diagonal contributions to the thermal diffusivity are generally small, better agreement can be achieved for $M\leqslant 10$ if they are included. In particular, these off-diagonal contributions are $O(1/M^2)$. They have been calculated explicitly in two dimensions in Ref. [3], and for model B in Sec. IV A 2 of this paper.

3. Self-diffusion coefficient

The self-diffusion constant D of particle i is defined by

$$D=\lim_{t\to\infty}\frac{1}{2dt}\langle[\mathbf{r}_i(t)-\mathbf{r}_i(0)]^2\rangle. \tag{50}$$

The position of the particle at time $t=n\tau$ is

$$\mathbf{r}_i(t)=\mathbf{r}_i(0)+\tau\sum_{i=0}^{n-1}\mathbf{v}_i(k\tau), \tag{51}$$

so that

$$\langle[\mathbf{r}_i(t)-\mathbf{r}_i(0)]^2\rangle=\tau^2\sum_{j=0}^{n-1}\sum_{k=0}^{n-1}\langle\mathbf{v}_i(j\tau)\cdot\mathbf{v}_i(k\tau)\rangle. \tag{52}$$

The sums can be rewritten as

$$\sum_{j=0}^{n-1}\sum_{k=0}^{n-1}\langle\mathbf{v}_i(j\tau)\cdot\mathbf{v}_i(k\tau)\rangle$$

$$=\sum_{j=0}^{n-1}\langle\mathbf{v}_i^2(j\tau)\rangle+2\sum_{j=0}^{n-2}\sum_{k=j+1}^{n-1}\langle\mathbf{v}_i(j\tau)\cdot\mathbf{v}_i(k\tau)\rangle$$

$$=nd\,k_BT+2\sum_{j=1}^{n-1}j\langle\mathbf{v}_i(0)\cdot\mathbf{v}_i((n-j)\tau)\rangle. \tag{53}$$

Expression (53) can be evaluated using the same approximations as were used to determine the viscosity and thermal diffusivity. Setting $d=3$ and using Eq. (16), one gets

$$\langle\mathbf{v}_i(0)\cdot\mathbf{v}_i(k\tau)\rangle=3k_BT\gamma^k, \tag{54}$$

where

$$\gamma=[2\cos(\alpha)+1]/3-2[\cos(\alpha)-1]/(3M). \tag{55}$$

Substituting Eq. (54) into Eq. (53), one gets

$$D=\lim_{n\to\infty}k_BT\tau\left[\frac{1}{2}+\frac{1}{n}\sum_{j=1}^{n-1}j\gamma^{n-j}\right]=\frac{k_BT\tau}{2}\left[\frac{1+\gamma}{1-\gamma}\right], \tag{56}$$

or, explicitly, as a function of M,

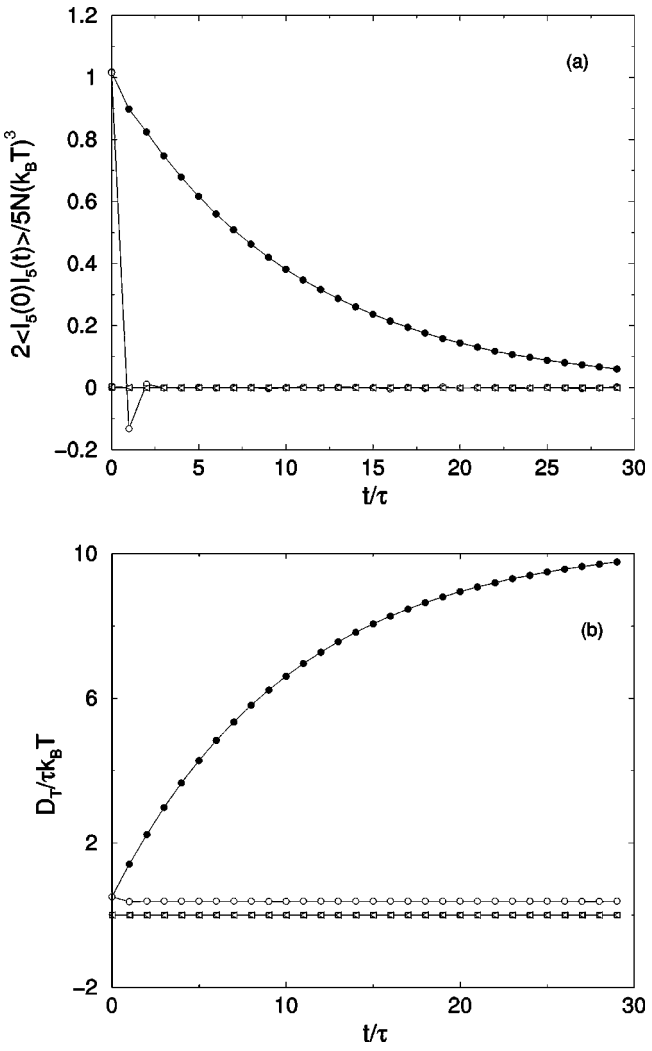

FIG. 6. (a) Normalized correlation functions $2\langle I_5(0)I_5(t)\rangle/5N(k_BT)^3$ for model A as a function of time for $\alpha=30°$ (filled symbols) and $\alpha=150°$ (unfilled symbols). For $\alpha=30°$, the kinetic, rotational, and mixed contributions are indicated by ●, ■, and ◀, respectively. For $\alpha=150°$, the kinetic, rotational, and mixed contributions are indicated by ○, □, and ◁, respectively. (b) Normalized time dependent thermal diffusivity, $D_T(t)/\tau k_BT$. Symbols are the same as in part (a). Parameters: $L/a=32$, $\lambda/a=2.309$, $\tau=1$, and $M=20$. The data were obtained by time averaging over 75 000 iterations.

$$D=\frac{k_BT\tau}{2}\left[\frac{3}{1-\cos(\alpha)}\left(\frac{M}{M-1}\right)-1\right]. \tag{57}$$

The diffusion coefficient was measured for $M=5$ and 20 and $\lambda/a=2.309$; the results are shown in Fig. 8.

B. Shear viscosity at small mean free path approximation

Simple kinetic arguments can be used to calculate the rotational contribution to the kinematic viscosity [2]. Consider a collision cell of linear dimension a and divide the cell by the plane $z=h$. Since the particle collisions occur in a shifted cell coordinate system, they result in a transfer of momentum between neighboring cells in the unshifted reference frame. The plane $z=h$ represents a cell boundary in the unshifted frame. Consider now the momentum transfer in the z direction, and assume a homogeneous distribution of particles in the cell. The mean velocities in the lower and upper partitions are

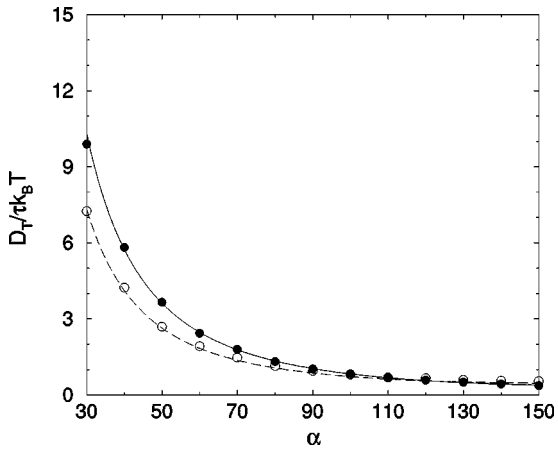

FIG. 7. Normalized thermal diffusivity $D_T/\tau k_BT$ for model A as a function of collision angle α. The lines are the theoretical prediction, Eq. (48). The data were obtained by time averaging over 75 000 iterations. Parameters: $L/a=32$, $\lambda/a=2.309$, $\tau=1$, and $M=5$ (○) and $M=20$ (●).

$$\mathbf{u}_1=\frac{1}{M_1}\sum_{i=1}^{M_1}\mathbf{v}_i \tag{58}$$

and

$$\mathbf{u}_2=\frac{1}{M_2}\sum_{i=M_1+1}^{M}\mathbf{v}_i, \tag{59}$$

respectively, where $M_1=M(a-h)/a$ and $M_2=Mh/a$. The x component of the momentum transfer resulting from the collision is

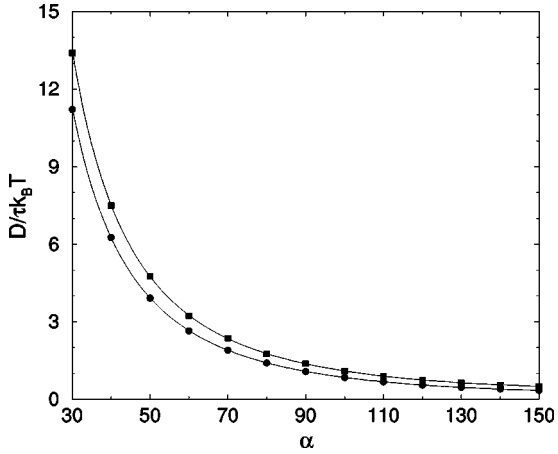

FIG. 8. Normalized self-diffusion constant $D/\tau k_BT$ for model A as a function of collision angle α. The lines are the theoretical prediction, Eq. (57). The data were obtained by time averaging over 75 000 iterations. Parameters: $L/a=32$, $\lambda/a=2.309$, $\tau=1$, and $M=5$ (■) and $M=20$ (●).

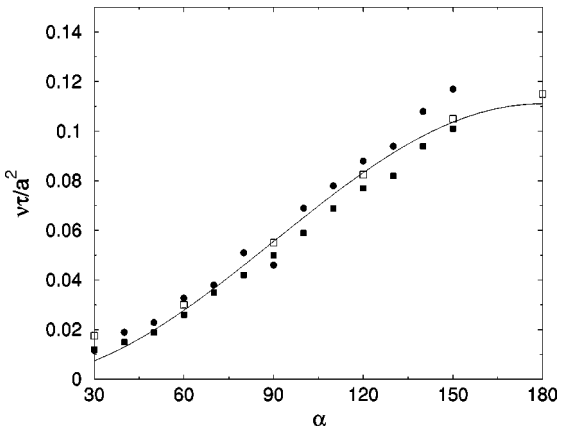

FIG. 9. Normalized kinematic viscosity for model A as a function of collision angle α for small mean free path, $\lambda/a=0.0361$. The plot shows both the rotational (●) and the total (■) contributions to the viscosity. The solid line is the theoretical prediction, Eq. (34). The data were obtained by time averaging over 75 000 iterations. Parameters: $L/a=32$ and $M=20$. The open squares (□) are data for the total kinematic viscosity obtained in Ref. [8].

$$\Delta p_x(h)\equiv\sum_{i=1}^{M_1}\left[v_{i,x}(t+\tau)-v_{i,x}(t)\right]. \tag{60}$$

Using Eq. (20) and averaging over the orientation of the vector $\hat{\mathbf{R}}$ then yields

$$\Delta p_x(h)=\frac{2}{3}(c-1)M_1(u_{1,x}-u_x). \tag{61}$$

Since $M\mathbf{u}=M_1\mathbf{u}_1+M_2\mathbf{u}_2$,

$$\Delta p_x(h)=\frac{2}{3}(1-c)M(u_{2,x}-u_{1,x})\frac{h}{a}\left(1-\frac{h}{a}\right), \tag{62}$$

so that and averaging over h—which corresponds to averaging over the random grid shift—one has

$$\langle\Delta p_x\rangle=\frac{1}{9}(1-c)M(u_{2,x}-u_{1,x}). \tag{63}$$

Since the dynamic viscosity η is defined as the ratio of the tangential stress P_{zx} to $\partial u_x/\partial z$, we have

$$\eta=\frac{\langle\Delta p_x\rangle/(a^2\tau)}{\partial u_x/\partial z}=\frac{\langle\Delta p_x\rangle/(a^2\tau)}{(u_{2,x}-u_{1,x})/(a/2)}, \tag{64}$$

so that the kinematic viscosity $\nu=\eta/\rho$ is

$$\nu=\frac{a^2}{18\tau}[1-\cos(\alpha)] \tag{65}$$

in the limit of small mean free path.

We have measured both the rotational and total contributions to the kinematic viscosity for $\lambda/a=0.0361$. The results are shown in Fig. 9. As can be seen, multiparticle collisions provide the dominant contribution to the viscosity for small mean free path. Furthermore, Eq. (65) provides an accurate approximation for the viscosity in this regime. The systematic deviations for small α are due to kinetic contributions (see Fig. 4).

IV. MODEL B: ROTATION AROUND ORTHOGONAL AXES

The second collision rule we will consider involves rotations about one of three orthogonal axes. In the implementation considered here, we take these axes to be the *x*, *y*, and *z* axes of a Cartesian coordinate system. At each collision step, one of these axes is chosen at random, and a rotation by an angle $\pm\alpha$ is then performed about this axis. The sign of α is chosen with equal probability. Rotations about the *x*, *y*, and *z* axes are described by the rotation matrices

$$M_x=\begin{pmatrix}1&0&0\\0&c&s\\0&-s&c\end{pmatrix},\quad M_y=\begin{pmatrix}c&0&s\\0&1&0\\-s&0&c\end{pmatrix},$$

$$M_z=\begin{pmatrix}c&s&0\\-s&c&0\\0&0&1\end{pmatrix}, \tag{66}$$

where $c=\cos(\alpha)$ and $s=\pm\sin(\alpha)$, depending on the sign of α. In the following, we will refer to this collision rule as model B. The rate of approach to thermal equilibrium for this model is almost identical to that of model A. This can be seen in Fig. 2, which shows the angular dependence of τ_R/M for two values of λ/a, 1.15 (●) and 0.0361 (□). As in two dimensions, the relaxation rate is essentially independent of temperature.

An advantage of model B is that the analytical calculations are comparatively simple and resemble those for the model in two dimensions. However, as will be shown in the following section, there are new finite cell size corrections which are unique to this collision rule. As will be shown, they occur because rotations are performed about one of the symmetry axes of the cell lattice.

A. Large mean free path approximation

1. Shear viscosity

For large mean free path, we proceed as in Sec. III A 1. In order to determine the shear viscosity in this regime, we need to evaluate temporal correlation functions of the type

$$A_n=\sum_{ij}\langle v_{ix}(0)x_{iy}(0)v_{jx}(n\tau)v_{jy}(n\tau)\rangle. \tag{67}$$

A_0 has the same value as in model A. For $n\neq 0$, there are again both diagonal ($j=i$) and off-diagonal ($j\neq i$) contributions to A_n. Using the definition of the rotation matrices, Eq. (66), it is easy to show the diagonal contributions to A_1:

$$A_1^x=N(k_BT)^2\zeta_1, \tag{68}$$

$$A_1^y=N(k_BT)^2\zeta_1, \tag{69}$$

and

$$A_1^z = N(k_B T)^2(\zeta_1^2 - \zeta_2^2), \tag{70}$$

for rotations around the x, y, and z axes, respectively, where $\zeta_1 = 1/M + c(1-1/M)$ and $\zeta_2 = s(1-1/M)$. Averaging over the three rotation axes, it follows that the total diagonal contribution is

$$\frac{1}{3}(A_1^x + A_1^y + A_1^z) = N(k_B T)^2 \zeta_B, \tag{71}$$

where

$$\zeta_B = (2\zeta_1 + \zeta_1^2 - \zeta_2^2)/3. \tag{72}$$

The off-diagonal contributions, which come from particles j which are in the same cell as particle i at $t=0$, can be evaluated in a similar fashion. The result is

$$N(k_B T)^2 (M-1)\,\eta_B, \tag{73}$$

where $\eta_B = 2c(c-1)/(3M^2)$, so that

$$A_1 = N(k_B T)^2[\zeta_B + (M-1)\,\eta_B]. \tag{74}$$

The off-diagonal contribution is three times smaller than in two dimensions [3]. Note that the leading diagonal contribution is $O(1)$, while that of the off-diagonal contribution is $O(1/M)$.

The behavior over longer time intervals can be analyzed in a similar fashion, and as for model A, one finds

$$A_n = N(k_B T)^2[\zeta_B + (M-1)\,\eta_B]^n, \tag{75}$$

so that

$$\nu = \frac{k_B T\,\tau}{2}\left(\frac{1+\zeta_B+\eta_B}{1-\zeta_B-\eta_B}\right) + w_B\left(c, \frac{a^2}{\tau}\right). \tag{76}$$

The last term on the right hand side of Eq. (76) is a finite cell size correction. In two dimensions and for model A, $w_A = a^2/(12\tau)$ [3]. As discussed in Sec. III A 1, it occurs because the substitution $\Delta\xi_{iy} = \tau v_{iy}$ in the first term on the sum on the right hand side of Eq. (8) is not precisely correct. In the present case, however, there are additional corrections because the rotation matrices always leave one component of the velocity unaltered. As a result, there are contributions to C_1 that have projections on C_0.

Finite cell size correction. In order to simplify the discussion of the finite cell size corrections, the following calculations are performed in the limit $M \to \infty$. In this case, the time evolution equations reduce to

$$v_{ix}(\tau) = v_{ix}(0),$$

$$v_{iy}(\tau) = c v_{iy}(0) + zs v_{iz}(0) \tag{77}$$

for rotations around the x axis,

$$v_{ix}(\tau) = c v_{ix}(0) + zs v_{iz}(0),$$

$$v_{iy}(\tau) = v_{iy}(0) \tag{78}$$

for rotations around the y axis, and

$$v_{ix}(\tau) = c v_{ix}(0) + zs v_{iy}(0),$$

$$v_{iy}(\tau) = c v_{iy}(0) - zs v_{ix}(0) \tag{79}$$

for rotations around the z axis, where as before, c and s are the cosine and the sine of the rotation angle α. $z = \pm 1$ specifies the sign of α.

When calculating C_1, we have to consider rotations about the three symmetry axes separately. As can be seen from Eqs. (79), rotations about the z axis mix both the x and y components of the velocity, so that the situation is similar to that considered in Sec. II B 4 of Ref. [3]. Although the same techniques can be used to evaluate C_1^z as in Ref. [3], we know from the results of that paper that there are no finite cell size corrections in this case.

The situation is different for rotations about the x and y axes. For rotations about the x axis, one has

$$\tau^2 C_1^x = k_B T \sum_i \langle \Delta\xi_{iy}(0)\Delta\xi_{iy}(\tau)\rangle, \tag{80}$$

so that $\langle \Delta\xi_{iy}(0)\Delta\xi_{iy}(\tau)\rangle$ needs to be evaluated. Using the approach described in Sec. II B 4 of Ref. [3], we have

$$\tau^2 C_1^x / N k_B T = a \int_0^a dy_0 \sum_{n,m=-\infty}^{\infty} \int_{(na-y_0)/\tau}^{[(n+1)a-y_0]/\tau} dv_y \times \int_{b_0}^{b_1} dv_z\, nm\, w(v_x) w(v_z), \tag{81}$$

where all velocities are at equal time, so that we have dropped the argument (0). Note that the average over $z = \pm 1$ has already be performed. The limits on the inner integral are

$$b_0 = [(m+n)a - y_0 - v_y(1+c)\tau]/(s\tau) \tag{82}$$

and

$$b_1 = [(m+n+1)a - y_0 - v_y(1+c)\tau]/(s\tau). \tag{83}$$

$w(v_x)$ is the Boltzmann distribution,

$$w(v_x) = \frac{1}{\sqrt{2\pi k_B T}} \exp\left\{-\frac{v_x^2}{2k_B T}\right\}. \tag{84}$$

Equation (81) looks very similar to Eqs. (18) and (41) in Ref. [3] and can be evaluated in an analogous fashion. We therefore only sketch the main steps of the analysis, referring to Ref. [3] for details.

The Poisson sum formula [18]

$$\sum_{n=-\infty}^{\infty} g(n) = \sum_{m=-\infty}^{\infty} \int_{-\infty}^{\infty} g(\phi) e^{-2\pi i m\phi} d\phi \tag{85}$$

is first used twice to transform the double sum over m and n in Eq. (81). Partial integrations over v_x and v_z are then performed. The temperature independent part of the resulting expression can be determined by evaluating the $\bar{m}=\bar{n}=0$ contribution of the remaining sums. The final result of these calculations is

$$\tau^2 C_1^x / N k_B T = -\frac{a^2}{12} + O(k_B T). \tag{86}$$

For rotations about the y axis, one has

$$\tau^2 C_1^y = k_B T\, c \sum_i \langle \Delta\xi_{iy}(0)\Delta\xi_{iy}(\tau)\rangle. \tag{87}$$

In this case, $v_{iy}(\tau)=v_{iy}(0)$, and the calculation of $\langle \Delta\xi_{iy}(0)\Delta\xi_{iy}(\tau)\rangle$ can be performed using the methods outlined above. The final result is

$$\tau^2 C_1^y / N k_B T = -c\frac{a^2}{12} + O(k_B T). \tag{88}$$

Averaging over all three different rotation axes, it follows that

$$\tau^2 C_1 / N k_B T = -\frac{a^2}{36}(1+c) + O(k_B T). \tag{89}$$

Adding this to the contribution from C_0, the final approximation for the finite cell size correction for model B is

$$w_B(c, a^2/\tau) = \frac{a^2}{18\tau}\left(1-\frac{c}{2}\right). \tag{90}$$

Although this result is obtained for $M\to\infty$, and neglects contributions from C_n with $n\geqslant 2$, it reproduces the behavior of the viscosity over rotation angles between 10° and 140° and $\lambda/a > 0.5$ with an error smaller than 2%.

For $M\to\infty$, the off-diagonal contributions to the viscosity vanish, and the kinematic viscosity has a minimum at $\alpha = 120°$ for $\lambda/a\to\infty$. For this value of α,

$$\nu_{min}^B = \tau k_B T\left[\frac{1}{6}+\frac{5}{72}\left(\frac{a}{\lambda}\right)^2\right]. \tag{91}$$

This is significantly smaller than the minimum value given in Eq. (35) for model A, but still larger than the minimum value in two dimensions, Eq. (36).

Figure 10 contains a plot of the normalized kinematic viscosity $\nu/(\tau k_B T)$ as a function of α for $\lambda/a = 1.15$ and $M=20$. Data for the the kinetic ($\times$) and rotational ($\square$) contributions, as well as the total ($\bullet$) viscosity, are plotted and compared with the theoretical prediction, Eqs. (76) and (90). The agreement is excellent. Note, in particular, that the finite cell size contribution to the total viscosity is not negligible, particularly for large rotation angles. In Fig. 11, the normalized viscosity $\nu/(\tau k_B T)$ is plotted as a function of M for $\alpha = 90°$ and $\lambda/a = 1.15$. Again, the agreement between theory and simulation is excellent. Finally, Fig. 12 shows the normalized total shear viscosity $\nu\tau/a^2$ as a function of

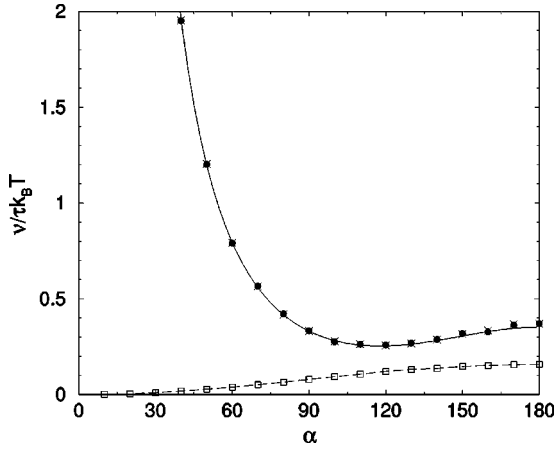

FIG. 10. Various contributions to the normalized shear viscosity $\nu/\tau k_B T$ for model B as a function of the rotation angle α at large mean free path, $\lambda/a = 1.15$. The symbols are simulation data for the kinetic contribution ($\times$), the rotational contribution ($\square$), and the total viscosity ($\bullet$). The solid line is the theoretical prediction, Eqs. (76) and (90). The viscosity has a minimum at $\alpha = 120°$, as predicted by theory. The data were obtained by time averaging over 40 000 iterations. Parameters: $L/a = 32$, $\tau = 1$, and $M = 20$.

$(\lambda/a)^2$ for $M=20$ and $\alpha = 90°$. Note, in particular, that both the M dependence of the viscosity as well as the size of the finite cell size correction—given by the intercept—are accurately described by theory.

2. Thermal diffusivity

The kinetic part of the reduced flux for the calculation of the thermal diffusivity is given by Eq. (38), where again, $B_n \equiv \langle I_5^{kin}(\hat{\mathbf{z}},0)|I_5^{kin}(\hat{\mathbf{z}},n\tau)\rangle$. The calculation of the thermal diffusivity simplifies considerably if we utilize relation (39) and the following relations:

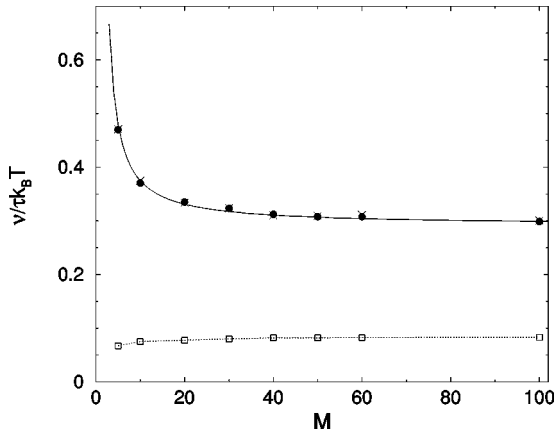

FIG. 11. Various contributions to the normalized shear viscosity $\nu/\tau k_B T$ for model B as a function of M for large mean free path, $\lambda/a = 1.15$, and $\alpha = 90°$. The symbols are simulation data for the kinetic contribution ($\times$), the rotational contribution ($\square$), and the total viscosity ($\bullet$). The solid line is the theoretical prediction, Eqs. (76) and (90). For this value of λ/a, rotational contributions to the total viscosity are negligible.

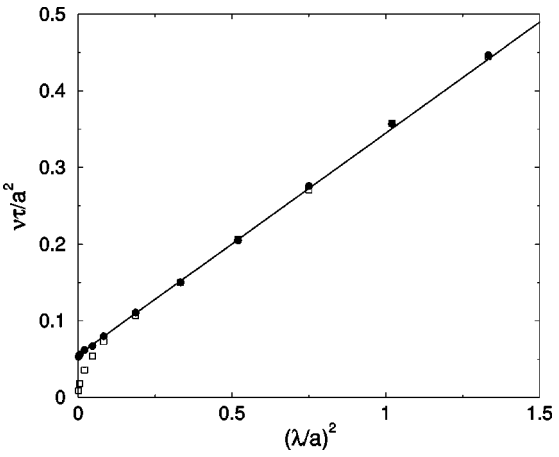

FIG. 12. Shear viscosity for model B as a function of λ/a for $\alpha=90°$ and $M=20$. The symbols are simulation data for the kinetic contribution (□) and the total viscosity (●). The slope of 0.297 is in excellent agreement with the theoretical prediction, 0.2895, which follows from Eqs. (76) and (90). Note that for $M\to\infty$, theory predicts a slope of 0.25; $1/M$ corrections are therefore important even for $M=20$. Parameters: $L/a=32$, $\tau=1$.

$$\left\langle \left(c_p T - \frac{v_i^2(t)}{2} \right) v_{ix}^m \right\rangle = 0 \quad \text{for} \quad m=1, 2, \text{and } 3, \tag{92}$$

$$\left\langle \left(c_p T - \frac{v_i^2(t)}{2} \right) v_{ix}^4 \right\rangle = 3(k_B T)^3, \tag{93}$$

and

$$\left\langle \left(c_p T - \frac{v_i^2(t)}{2} \right) v_{ix}^2 v_{iy}^2 \right\rangle = (k_B T)^3. \tag{94}$$

B_0 is the same as in model A, namely,

$$B_0 = \frac{5}{2} N (k_B T)^3. \tag{95}$$

B_1 (including off-diagonal terms) is

$$B_1 = \frac{5}{2} N (k_B T)^3 [\gamma\gamma_4 + (M-1)\gamma_5], \tag{96}$$

where γ is given given in Eq. (55),

$$\gamma_4 = [1 + 2(\zeta_1^2 + \zeta_2^2)]/3, \tag{97}$$

where ζ_1 and ζ_2 are defined in the text following Eq. (70), and

$$\gamma_5 = \frac{16}{15} \frac{(1-c)^2}{M^3}. \tag{98}$$

The coefficients B_n form a geometrical series, because successive rotations are uncorrelated. This can be seen by *first* performing an average over the rotation angle and *then* performing the thermal average. In particular,

$$B_n = \frac{5}{2} N (k_B T)^3 [\gamma\gamma_4 + (M-1)\gamma_5]^n, \tag{99}$$

so that the thermal diffusivity is

$$D_T = \frac{k_B T \tau}{2} \left[\frac{1 + \gamma\gamma_4 + (M-1)\gamma_5}{1 - \gamma\gamma_4 - (M-1)\gamma_5} \right]. \tag{100}$$

Note that the off-diagonal contribution is of order $1/M^2$; it is therefore less important than for the shear viscosity.

3. Self-diffusion coefficient

The diffusion constant can be determined as in Sec. III A 2 for model A. The final result is

$$D = \frac{k_B T \tau}{2} \left(\frac{1+\gamma}{1-\gamma} \right), \tag{101}$$

which is the same as for model A [see Eq. (57)]. It is interesting to note that

$$\frac{D_T}{D} \to 1 \quad \text{for } M \to \infty, \tag{102}$$

for both models A and B as well as in two dimensions.

B. Small mean free path approximation: Shear viscosity

A detailed calculation of the shear viscosity in this limit can be performed following the arguments used in Sec. III A 2 for model A and in Ref. [3] for two dimensions. However, for model B, the following simple argument gives the same result. Consider the momentum transfer across a plane perpendicular to the z axis. Only rotations about the x and y axes produce a nonzero momentum transfer, and since the momentum transfer—and therefore the resulting viscosity—from each of these rotations is equal to that calculated two-dimensions [3], one finds that

$$\nu_{3D} = \frac{2}{3} \nu_{2D} = \frac{a^2}{18\tau} [1 - \cos(\alpha)]. \tag{103}$$

Note that this expression is identical to the one obtained for model A. Data for the α dependence of the normalized viscosity, $\nu\tau/a^2$, at $\lambda/a=0.0361$ are plotted in Fig. 13. Note, in particular, the importance of kinetic contributions to the viscosity for small α, even for this small value of λ/a.

V. SUMMARY

In this paper we have presented a comprehensive analytical and numerical study of the stochastic rotation dynamics model for fluid dynamics in three dimensions for two collision rules. The first collision rule (model A) consists of a rotation by an angle α about a randomly chosen axis. It was introduced in Refs. [4] and [5] and used in Ref. [8] to study channel flow and flow about a spherical object. A new, simpler collision rule (model B), in which collisions involve rotations by an angle $\pm\alpha$ about one of three orthogonal axes, was also discussed. Calculations involving this model are

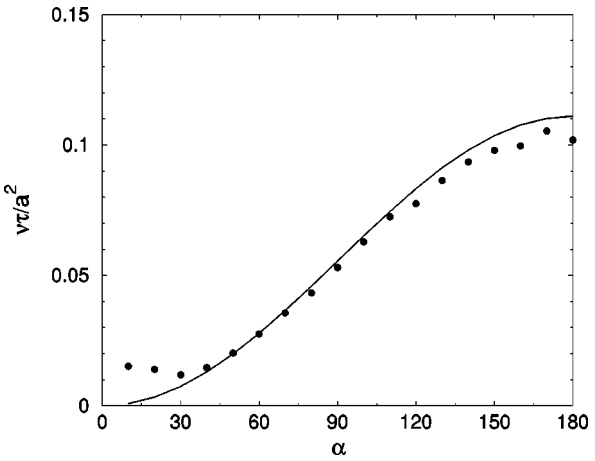

FIG. 13. Normalized shear viscosity $\nu\tau/a^2$ for model B as a function of the rotation angle α for small mean free path, $\lambda/a = 0.0361$. The bullets are simulation data and the solid line is the theoretical prediction, Eq. (103), for the rotational contribution to the kinematic viscosity. The deviation of the data from the theoretical prediction for $\alpha < 30°$ is due to the increasing importance of the kinetic contribution to the viscosity (see Fig. 10). The data were obtained by time averaging over 40 000 iterations. Parameters: $L/a = 32$, $\tau = 1$, and $M = 20$.

particularly simple, since the rotations about the individual axes are very similar to those in two dimensions. In particular, it was possible using this model to calculate the off-diagonal contributions to the thermal diffusivity; a similar calculation for model A was prohibitively tedious. Since both models are comparable with regard to their computational efficiency, i.e., relaxation rates, range of viscosities, etc., the simplicity of model B can have advantages in specific applications.

Discrete time Green-Kubo relations originally derived in Refs. [1] and [2] were used to determine explicit expressions for the shear viscosity, the thermal diffusivity, and the self-diffusion constant. The kinetic, collision, and mixed contributions to the transport coefficients were analyzed individually, and no assumptions regarding molecular chaos were made. This enabled us to determine correlation induced finite cell size corrections to the shear viscosity which persist even in the limit of large mean free path. In Ref. [3] it was shown that these corrections can, under certain circumstances, such as collisions with $\alpha = 90°$ and large particle density, provide the dominant contribution to the shear viscosity in two dimensions. In three dimensions, we showed here that corrections of this type, while not entirely negligible, are rather small for model A. However, as discussed in Sec. IV A 1, for model B, where collisions involve rotations about one of three previously defined orthogonal axes, there are additional finite cell size corrections that make non-negligible contributions to the viscosity for a wide range of densities and rotation angles. It is important to note that corrections of this type are only important for the shear viscosity.

It was also shown how quaternion algebra can be used to simplify calculations of kinetic contributions to the transport coefficients. In particular, the appendixes describe the calculation of the thermal diffusivity in model A using quaternions. Finally, simulation results for the viscosity, thermal diffusivity, and the self-diffusion coefficient for a range of simulation parameters were presented and compared to the analytical approximations. In all cases, agreement was excellent; furthermore, the comparisons showed that the finite cell size corrections described above are necessary in order to achieve quantitative agreement.

ACKNOWLEDGMENTS

Support from the National Science Foundation under Grant No. DMR-0083219, the donors of The Petroleum Research Fund, administered by the ACS, the Deutsche Forschungsgemeinschaft under Project No. 214283, and Sonderforschungsbereich 404 is gratefully acknowledged. We thank E. Allahyarov and G. Gompper for providing results of their viscosity measurements published in Ref. [8].

APPENDIX A

The calculation of correlation functions of the reduced fluxes can be simplified by rewriting the time evolution equations for the velocities using quaternions. Two arbitrary quaternions, $\mathbb{P}$ and $\mathbb{Q}$, are defined by

$$\mathbb{P} \equiv (p, \mathbf{P}), \tag{A1}$$

$$\mathbb{Q} \equiv (q, \mathbf{Q}), \tag{A2}$$

where $\{p,q\}$ are the scalar parts and $\{\mathbf{P},\mathbf{Q}\}$ the corresponding vector parts of the quaternions. If the scalar part is zero, the quaternion is an ordinary vector and is called as a ''pure'' quaternion. The multiplication rule of two quaternions is given by [19]

$$\mathbb{P}\mathbb{Q} \equiv (pq - \mathbf{P}\cdot\mathbf{Q},\ \ p\mathbf{Q} + q\mathbf{P} + \mathbf{P}\times\mathbf{Q}). \tag{A3}$$

It follows that for two pure quaternions, $\mathbb{R} \equiv (0,\mathbf{R})$ and $\mathbb{S} \equiv (0,\mathbf{S})$,

$$\mathbb{R}\mathbb{S}\mathbb{R} = (0, -|\mathbf{R}|^2\mathbf{S}). \tag{A4}$$

Defining

$$\mathbb{V}(t) \equiv (0,\mathbf{v}(t)), \tag{A5}$$

$$\mathbb{U} \equiv (0,\mathbf{u}_{\xi}), \tag{A6}$$

and

$$\mathbb{V}^r \equiv (0,\mathbf{v}^{\mathbf{r}}) \equiv \mathbb{V}(0) - \mathbb{U}. \tag{A7}$$

The time evolution equation for the velocities, Eq. (16), can be written as

$$\mathbb{V}(\tau) = \mathbb{A}\mathbb{V}^r\mathbb{A}^* + \mathbb{U}, \tag{A8}$$

where

$$\mathbb{A} \equiv (\cos(\alpha/2), \hat{\mathbf{R}}\sin(\alpha/2)). \tag{A9}$$

The first term in Eq. (A8) corresponds to the rotation of the relative velocity vector around the random axis $\hat{\mathbf{R}}$. Using the multiplication rule given in Eq. (A3), it is easy to see that Eq. (A8) is equivalent to Eq. (16). Similarly, using Eq. (A4) it can be shown that

$$(\mathbb{V}^3(\tau))_z = -v^2(\tau)v_z(\tau). \tag{A10}$$

Dropping the index i, B_1 given by Eq. (41) can be written as

$$\frac{B_1}{N} = \underbrace{\frac{1}{4}\langle v^2 v^2(\tau)v_z(\tau)v_z\rangle}_{B_1'} - \underbrace{\frac{c_p T}{2}\langle v^2(\tau)v_z(\tau)v_z\rangle}_{B_1''}, \tag{A11}$$

or by using Eq. (A10), as

$$\frac{B_1}{N} = \frac{1}{4}\langle(\mathbb{V}^3(\tau))_z v_z(v_x^2+v_y^2+v_z^2)\rangle - \frac{c_p T}{2}\langle(\mathbb{V}^3(\tau))_z v_z\rangle. \tag{A12}$$

Using the multiplication rule for quaternions, and the fact that $\mathbb{A}\mathbb{A}^*=1$, it can be shown that

$$\mathbb{V}^3(\tau) = \mathbb{A}(\mathbb{V}^r)^3\mathbb{A}^* + \mathbb{U}^2\mathbb{A}\mathbb{V}^r\mathbb{A}^* + \mathbb{A}\mathbb{V}^r\mathbb{A}^*\mathbb{U}\mathbb{A}\mathbb{V}^r\mathbb{A}^* + \mathbb{U}\mathbb{A}(\mathbb{V}^r)^2\mathbb{A}^* \tag{A13}$$

$$+ \mathbb{A}(\mathbb{V}^r)^2\mathbb{A}^*\mathbb{U} + \mathbb{U}^3 + \mathbb{A}\mathbb{V}^r\mathbb{A}^*\mathbb{U}^2 + \mathbb{U}\mathbb{A}\mathbb{V}^r\mathbb{A}^*\mathbb{U}. \tag{A14}$$

Simplifying terms and using energy conservation,

$$\sum_\alpha [v_\alpha^r(\tau)]^2 - [v_\alpha^r]^2 = 0, \tag{A15}$$

one obtains

$$B_1' = \frac{1}{4}\langle\{v_x^2+v_y^2+v_z^2+2u_{\xi x}[v_x(\tau)-v_x]+2u_{\xi y}[v_y(\tau)-v_y] + 2u_{\xi z}[v_z(\tau)-v_z]\}(v_x^2+v_y^2+v_z^2)v_z(\tau)v_z\rangle \tag{A16}$$

$$= \frac{(k_BT)^3}{12}\left\{35(1+2c) + \frac{2(1-c)}{M}\left[31-16c + \frac{20}{M}(2c-1)\right] + \frac{576(1-c)^2}{5M^3}\right\}. \tag{A17}$$

and

$$B_1'' = \frac{c_p T}{2}\langle\{v_x^2+v_y^2+v_z^2+2u_{\xi x}[v_x(\tau)-v_x] + 2u_{\xi y}[v_y(\tau)-v_y]+2u_{\xi z}[v_z(\tau)-v_z]\}v_z(\tau)v_z\rangle \tag{A18}$$

$$= \frac{5(k_BT)^3}{12}\left[5(1+2c) + \frac{10}{M}(1-c) - \frac{16}{5M^2}(1-c)^2\left(1-\frac{4}{M}\right)\right], \tag{A19}$$

which then yields Eq. (42) when substituted into Eq. (A11).

APPENDIX B

In the limit $M\to\infty$, $\mathbb{U}\to(0,\mathbf{0})$, and Eq. (A8) can be written as

$$\mathbb{V}(\tau) = \mathbb{A}\mathbb{V}\mathbb{A}^*, \tag{B1}$$

where we have dropped the superscript "**r**," so that $\mathbb{V} \equiv \mathbb{V}(0)$. The cube of $\mathbb{V}(\tau)$ is then simply

$$\mathbb{V}^3(\tau) = \mathbb{A}\mathbb{V}^3\mathbb{A}^*, \tag{B2}$$

where

$$\mathbb{V}^3 = (0, -|\mathbf{v}|^2\mathbf{v}). \tag{B3}$$

This means that $\mathbb{V}^3(\tau)$ is the rotation of the vector $-|\mathbf{v}|^2\mathbf{v}$ around a random axis $\hat{\mathbf{R}}$. Equations (B2) and (B3) can be used to evaluate the second term in Eq. (A11), namely,

$$E_1 \equiv \frac{2B_1''}{c_pT} = \langle v^2(\tau)v_z(\tau)v_z\rangle = -\langle(\mathbb{A}\mathbb{V}^3\mathbb{A}^*)_z v_z\rangle, \tag{B4}$$

which can be shown to equal

$$E_1 = 5(k_BT)^2\left[\frac{2\cos(\alpha)+1}{3}\right]. \tag{B5}$$

Similarly, for $t=2\tau$,

$$\mathbb{V}(2\tau) = \mathbb{A}'\mathbb{V}(\tau)\mathbb{A}'^*, \tag{B6}$$

where prime denotes a different random vector then in Eq. (A9). Using energy conservation and the commutator

$$[\mathbb{A}', \mathbb{V}] = [0, 2\sin(\alpha/2)\hat{\mathbf{R}}'\times\mathbf{v}], \tag{B7}$$

$\mathbb{V}^3(2\tau)$ can be written as

$$\mathbb{V}^3(2\tau) = -|\mathbf{v}(2\tau)|^2\mathbb{V}(2\tau) \tag{B8}$$

$$= -|\mathbf{v}(\tau)|^2\mathbb{A}'\mathbb{V}(\tau)\mathbb{A}'^* \tag{B9}$$

$$= -|\mathbf{v}(\tau)|^2(\mathbb{V}\mathbb{A}' + [\mathbb{A}', \mathbb{V}])\mathbb{A}'^* \tag{B10}$$

$$= -|\mathbf{v}(\tau)|^2\mathbb{V} - |\mathbf{v}(\tau)|^2\left(0, 2\sin\frac{\alpha}{2}\hat{\mathbf{R}}'\times\mathbf{v}\right)\mathbb{A}'^*, \tag{B11}$$

so that

$$(\mathbb{V}^3(2\tau))_z = -v^2(\tau)v_z(\tau)\left[\frac{2\cos(\alpha)+1}{3}\right]. \quad \text{(B12)}$$

Since

$$E_2 \equiv \langle v^2(2\tau)v_z(2\tau)v_z\rangle = -\langle(\mathbb{V}^3(2\tau))_z v_z\rangle, \quad \text{(B13)}$$

one gets finally,

$$E_2 = \left[\frac{2\cos(\alpha)+1}{3}\right]E_1 = 5(k_BT)^2\left[\frac{2\cos(\alpha)+1}{3}\right]^2, \quad \text{(B14)}$$

so that the terms B_n'' form a geometric series. It can also be shown that the B_n' are terms in a geometric series, with the same angular dependence. The difference of these two terms is therefore also a geometric series.

[1] T. Ihle and D.M. Kroll, Phys. Rev. E **63**, 020201(R) (2001).
[2] T. Ihle and D.M. Kroll, Phys. Rev. E **67**, 066705 (2003).
[3] T. Ihle and D.M. Kroll, Phys. Rev. E **67**, 066706 (2003).
[4] A. Malevanets and R. Kapral, J. Chem. Phys. **110**, 8605 (1999).
[5] A. Malevanets and R. Kapral, J. Chem. Phys. **112**, 7260 (2000).
[6] A. Lamura, G. Gompper, T. Ihle, and D.M. Kroll, Europhys. Lett. **56**, 319 (2001).
[7] A. Lamura and G. Gompper, Eur. Phys. J. E **9**, 477 (2002).
[8] E. Allahyarov and G. Gompper, Phys. Rev. E **66**, 036702 (2002).
[9] A. Malevanets and J.M. Yeomans, Europhys. Lett. **52**, 231 (2000).
[10] A. Malevanets and J.M. Yeomans, Comput. Phys. Commun. **129**, 282 (2000).
[11] Y. Hashimoto, Y. Chen, and H. Ohashi, Comput. Phys. Commun. **129**, 56 (2000).
[12] T. Sakai, Y. Chen, and H. Ohashi, Comput. Phys. Commun. **129**, 75 (2000).
[13] T. Sakai, Y. Chen, and H. Ohashi, Phys. Rev. E **65**, 031503 (2002).
[14] T. Sakai, Y. Chen, and H. Ohashi, Colloids Surf., A **201**, 297 (2002).
[15] Y. Inoue, Y. Chen, and H. Ohashi, Comput. Phys. Commun. **142**, 114 (2001).
[16] Y. Inoue, Y. Chen, and H. Ohashi, J. Stat. Phys. **107**, 85 (2002).
[17] S.H. Lee and R. Kapral, Physica A **298**, 56 (2001).
[18] P.M. Morse and H. Feshbach, *Methods of Theoretical Physics* (McGraw-Hill, New York, 1953).
[19] S.L. Altman, *Rotations, Quaternions, and Double Groups* (Clarendon Press, New York, 1986).